X-ray diffraction studies on the lock-in phase transition of intramolecular hydrogen-bonded compound d-BrHPLN

X-ray diffraction studies on the lock-in phase transition of intramolecular hydrogen-bonded compound d-BrHPLN

I Tamura†¶, Y Noda†+ Y Kuroiwa‡, T Mochida§ and T Sugawara‖

† Research Institute for Scientific Measurements, Tohoku University, Katahira, Aoba-ku, Sendai 980–8577, Japan
‡ Department of Physics, Faculty of Science, Okayama University, Tsushima-naka, Okayama 700-8530, Japan
§ Department of Chemistry, Faculty of Science, Toho University, Miyama, Funabashi-shi, Chiba 274–8510, Japan
‖ Department of Basic Sciences, Graduate School of Arts and Sciences, The University of Tokyo, Komaba, Meguro-ku, Tokyo 153–8902, Japan

E-mail: `ynoda@rism.tohoku.ac.jp`

Abstract. The phase transitions of deuterated 5-bromo-9-hydroxyphenalenone (d-BrHPLN), which was characterized as an isolated intramolecular hydrogen-bonded system, have been investigated by low-temperature x-ray diffraction experiments. The temperature dependence of lattice constants showed anomalous behaviour at the phase transition points $T_C(= 22.8$ K) and $T_I(= 34.5$ K). Superlattice reflections were found at (h k+0.5 0) below T_C and they deviated from the commensurate position in the intermediate phase ($T_C < T < T_I$). The peak shift δ showed a thermal hysteresis and was pinned on the position deviated from the commensurate one after several thermal cycles, even below T_C. The cause of the pinning effect was attributed to the creation of an improper hydrogen configuration excited electronically by x-ray radiation.

1. Introduction

Hydrogen-bonded materials exhibit a large isotope effect on the phase transition temperatures by replacing hydrogen atoms with deuterium. So far, two contrasting models have been presented for this phenomenon. One is a 'tunnelling model' proposed by Blinc [1] and also by Tokunaga and Matsubara [2], and the other is a 'geometrical model' proposed by Ichikawa *et al* [3]. In the former model, the isotope effect is explained by the quantum nature of the hydrogen motion in a double minimum potential, while the latter model treats the hydrogen-bond length as the most important factor. The hydrogen-bond lengths of deuterium compounds are known to be slightly longer than those of hydrogen compounds in general, and therefore the slight structural difference is considered to cause the change of the transition temperatures.

In recent years, we have investigated the isotope effect of the isolated hydrogen-bonded system $K_3H(SO_4)_2$, which has no network of the hydrogen bond [4–8]. The unique point of this system is that $K_3H(SO_4)_2$ has no phase transitions, while $K_3D(SO_4)_2$ undergoes a phase transition at $T_C = 84$ K [9]. The position, the electron density distribution and the motion of the hydrogen and deuterium atoms, as well as the hydrogen-bond length, have been extensively

¶ Present address: Institute for Molecular Science, Myodaiji, Okazaki, Aichi 444-8585, Japan.
+ To whom correspondence should be addressed.

studied. In this simple system we observed the geometrical effect: the hydrogen-bond length of $K_3H(SO_4)_2$ was slightly shorter than that of $K_3D(SO_4)_2$. Furthermore, the hydrogen-bond length in $K_3H(SO_4)_2$ became shorter than the critical bond length at low temperatures and the potential for the hydrogen atom changed from a double minimum to a single minimum potential. For this reason, it is still very difficult to judge whether the tunnelling model is essentially important or not.

Recently, an intramolecular hydrogen-bonded compound 5-bromo-9-hydroxyphenalenone ($C_{13}H_7BrO_2$ abbreviated as BrHPLN) was synthesized as the next candidate to investigate the isotope effect. Since the hydrogen-bond length of this system is fixed by the molecular frame, it is expected that the hydrogen-bond lengths are the same for hydrogen and deuterium compounds. If the hydrogen-bond length is fixed for both compounds, the role of the geometrical effect should become clear. Furthermore, the existence of the tunnelling motion of the hydrogen atom is expected in this system [10]. Two energetically equivalent configurations of d-BrHPLN, in which a hydrogen atom relevant to the hydrogen bond is replaced with deuterium, are shown in figure 1. An x-ray crystallographic analysis [11] at room temperature showed that the molecules have no intermolecular hydrogen-bond network in the monoclinic unit cell (space group Cc or $C2/c$), and the hydrogen-bond length (the O–O distance) of BrHPLN is about 2.49 Å. Experiments of dielectric constants [12] revealed the existence of the phase transitions at 23 K and 34 K in d-BrHPLN, while a phase transition was not observed in BrHPLN: namely, this intramolecular hydrogen-bonded system shows an extraordinarily large isotope effect.
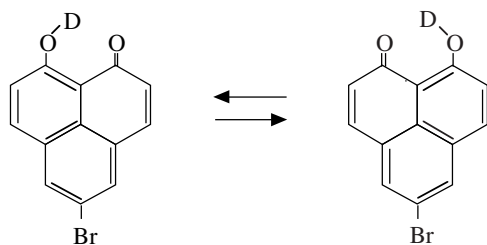

Figure 1. Two energetically equivalent configurations of d-BrHPLN molecules.

The concept 'hydrogen-bond length fixed by a molecular frame' is the keyword of this study. However, at the moment this is not established and we believe that it should be judged experimentally. We performed a conventional structure analysis of H and D compounds of BrHPLN at room temperature, and obtained results indicate that this idea is acceptable. The preliminary data are $R_{OO}(H) = 2.519(8)$ and $R_{OO}(D) = 2.505(11)$ Å, and the bond lengths seem to be equal within the experimental errors.

We reported in a preceding letter [13] that two phase transitions of d-BrHPLN correspond to the commensurate-to-incommensurate phase transition ($T_C = 22.8$ K) and the incommensurate-to-normal one ($T_I = 34.5$ K). In this paper we will present the detailed x-ray structural studies associated with the phase transitions of d-BrHPLN, referring to the temperature dependence of lattice constants, and the temperature dependence of the superlattice reflection. The origin of the pinning effect will also be discussed.

2. Experimental details

Single crystals of d-BrHPLN, with a typical sample dimension of $0.15 \times 0.15 \times 1.5$ mm³, were used for the x-ray diffraction experiment. A rotating anode x-ray generator with a Mo or a Cu target was operated with a power level of 50 kV$\times$60 mA. A fine-focused filament was used

and Kα radiation was monochromatized by PG(002). A newly developed x-ray apparatus [14] was applied to the low-temperature experiments and the counter and photographic methods were used simultaneously. This apparatus was composed of a double-axis diffractometer, a He-gas refrigerator-type cryostat and a curved image-plate. Weissenberg photographs were taken at low temperatures, and the Weissenberg photograph pattern was converted to a two-dimensional reciprocal-lattice pattern to survey weak superlattice reflections. The temperature dependence of the observed superlattice reflections was precisely investigated by the scintillation counter system.

3. Results

3.1. Temperature dependence of lattice parameters

Temperature dependence of lattice parameters was measured from 14.4 K to 282.6 K on heating, and the results are depicted in figure 2. The lattice parameters a, b, c and β exhibited anomalous behaviour at the phase transition temperatures, $T_C = 22.8$ K and $T_I = 34.5$ K, as shown in figure 2. On the other hand, the unit cell volume did not show any appreciable anomalies at T_C and T_I. Here, all parameters are referred to the unit cell of the room temperature phase, and do not necessarily represent the actual cells. In the preceding letter [13], we pointed out that the commensurate-to-incommensurate phase transition (T_C) was of first-order nature, and the incommensurate-to-normal phase transition (T_I) was of second-order. However, the discontinuous change of lattice constants, as is often observed in the first-order phase transitions, was not observed at T_C.

3.2. Search for superlattice reflections

In order to search for relevant superlattice reflections appearing at the low-temperature phases, oscillation and Weissenberg photographs were taken at 50 K and 14.4 K. The oscillation photographs were taken with the c-axis rotation, and no cell doubling was found along the c-axis direction. However, on the Weissenberg photograph of the ($h\,k\,0$) plane taken at 14.4 K by Cu Kα radiation, superlattice reflections were found. Figure 3 is the enlarged picture of the ($h\,k\,0$) reciprocal lattice at 14.4 K converted from the Weissenberg photograph. In the figure, large white spots correspond to the fundamental Bragg reflections forming the monoclinic lattice. Superlattice reflections were observed along the b^*-axis between the fundamental Bragg reflections. In the figure, (6 4.5 0), (5 5.5 0), (4 4.5 0) and (6 6.5 0) superlattice reflections appear intensively. On the picture taken at 50 K, these new reflections disappeared.

The Weissenberg photographs of the ($h\,0\,\ell$) plane were also taken at 14.4 K, and no superlattice reflection was found on this reciprocal plane. The lattice parameters at 14.4 K were $a = 12.050$ Å, $b = 23.426$ Å, $c = 6.927$ Å, $\beta = 98.4°$ and $Z = 8$, which indicates that the b-axis was doubled in the low-temperature phase. We found relatively intense $q = (0\,1/2\,0)$ type superlattice reflections, and the $2q$-positions where the Bragg intensity disappeared due to the C-lattice symmetry at the high temperature phase were extremely weak, roughly the background level in the present experiment but finite. We determined the 3D-space group of the commensurate phase as $P2_1/c$ from the consideration of the observed extinction rule.

3.3. Incommensurate nature of the superlattice reflections

Precise temperature dependence of the superlattice reflection was measured by the scintillation counter method. Figure 4 shows the profiles of the superlattice reflection (7 ζ 0) along the b^*-direction as a function of temperature. The data recorded during the first heating process
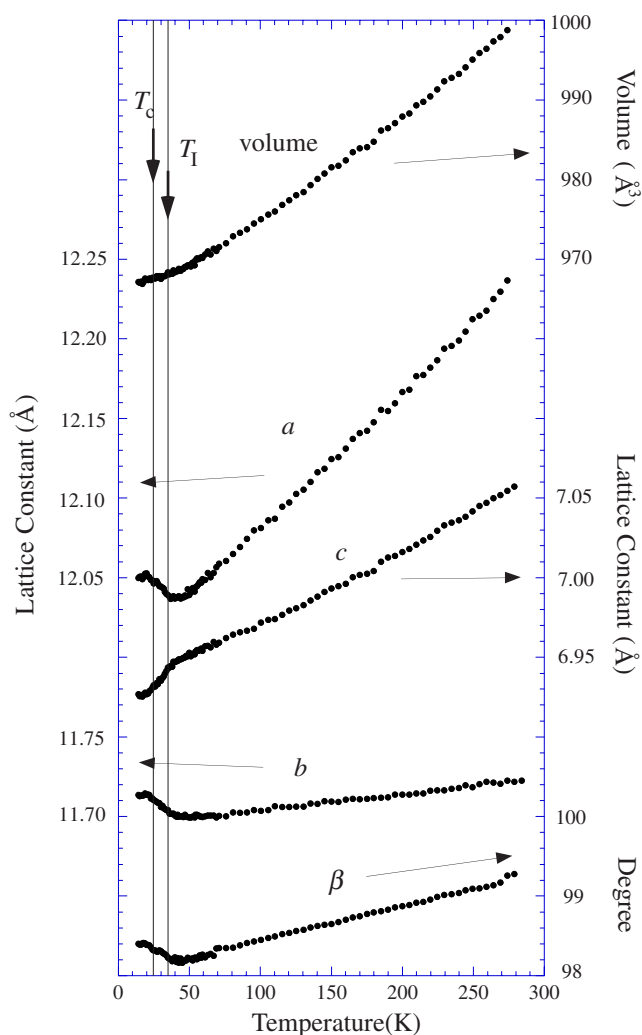
Figure 2. Temperature dependence of lattice parameters from 14.4 K to 282.6 K for the heating process. Anomalous behaviour is seen at $T_C = 22.8$ K and $T_I = 34.5$ K.

are given in figure 4(a) and those from the cooling process, after the heating process, are also given in figure 4(b).

When a virgin crystal was cooled down to 14.4 K, the superlattice reflection was observed at the position of approximately $\zeta = 0.5$ as shown in figure 4(a). The peak position remained at the same ζ value on heating up to 22.8 K. A new peak appeared abruptly at the position of $\zeta = 0.532$ at 22.8 K, coexisting with the peak at $\zeta = 0.5$. While the latter peak gradually disappeared with further increasing temperature, the position of the new peak moved along the b^*-direction. The peak shift δ, which was defined as $\zeta = 0.5 + \delta$ for representing the degree of the incommensurability, increased up to 34.5 K. Above 34.5 K the superlattice reflections became broad like a diffuse scattering.

The peak positions and the full widths at half maximum (FWHM) of the observed scattering profiles on the first heating process are shown in figure 5. In the figure, full circles
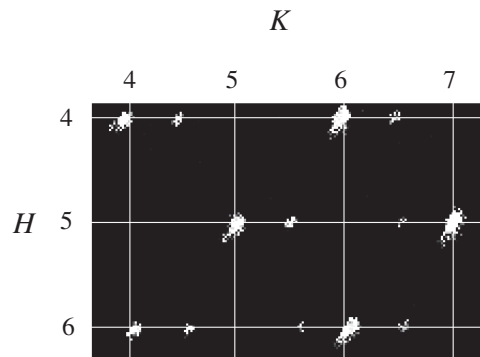
Figure 3. X-ray scattering intensity on the (h k 0) reciprocal lattice converted from the Weissenberg photograph taken at 14.4 K by using Cu Kα radiation.
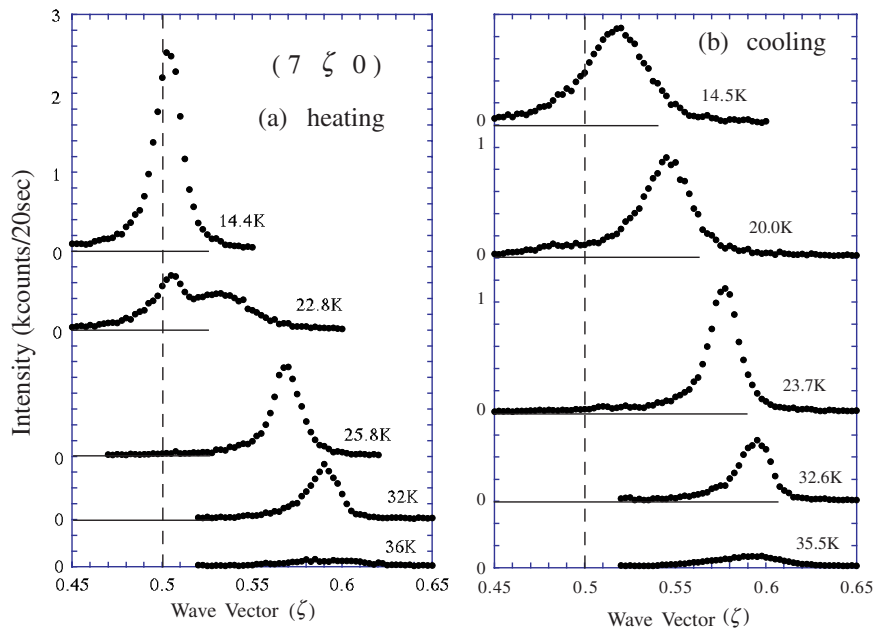

Figure 4. The profiles of the superlattice reflection (7 ζ 0) along the b^*-direction. (a) is for the first heating process and (b) is for the subsequent cooling process.

indicate the peak shifts δ, and bars indicate the FWHM of each profile. The instrumental resolution in FWHM is already corrected. As shown in the figure, the peak shift δ was unchanged in the temperature range from 14.4 K to 22.8 K, and the FWHM was essentially narrower than the resolution limit. The peak shift δ and the FWHM showed a discontinuous change at 22.8 K. These results demonstrate that the phase transition at $T_C = 22.8$ K was commensurate–incommensurate phase transition of the first-order and that at $T_I = 34.5$ K was incommensurate–normal phase transition of the second order.

After heating up to 41 K, the data on a cooling process were taken. The diffuse scattering became a superlattice reflection at lower temperature than 34.5 K, which is the same
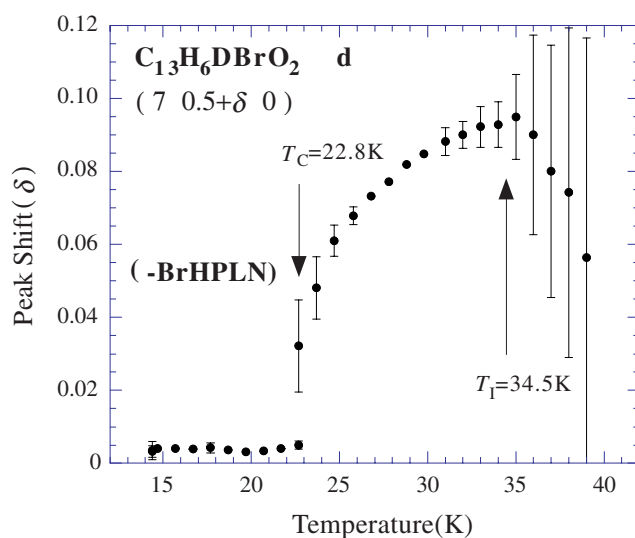
Figure 5. The peak positions δ and the FWHM along the b^*-direction of the superlattice reflection $(7\ 0.5+\delta\ 0)$ for the first heating process.

temperature as T_I in the heating process. On further cooling, the position of the superlattice reflection moved towards $\zeta = 0.5$ and finally it locked-in below 22.8 K. However, the lock-in position is not exactly $\zeta = 0.5$, and the peak shift δ still deviated from zero even down to 14.5 K as shown in figure 4(b). This phenomenon is usually called a pinning effect in which the lock-in position deviates from the exact commensurate one. The result contrasts with that in the first heating process (figure 4(a)). Besides, the width of the profile became extraordinarily broad. We show this point in more detail in the next subsection.

We also monitored the diffuse scattering above T_I. An intensity contour map together with a bird's eye view of the reciprocal space around $(7\ 0.5+\delta\ 0)$ measured at $T_I+1.1$ K are shown in figure 6. It is to be noted that the observed diffuse scattering is isotropical. The existence of the diffuse scattering at this reciprocal lattice point apparently indicates that the observed superlattice reflections represent the primary order parameter.

3.4. Hysteresis and radiation damage

As mentioned above, the lock-in position of the superlattice reflection at 14.4 K was not exactly at $\zeta = 0.5$ but slightly larger than 0.5. On the cooling process after the first heating, the shift δ increased furthermore. In order to clarify the origin of this pinning effect of the commensurate wave vector, we carefully monitored the superlattice reflection at around $(7\ 0.5\ 0)$ during four cycles of cooling and heating processes. The results are summarized in figure 7.

As shown in figure 7(a), the peak shift δ in the incommensurate phase falls on the same line for both the heating and the cooling processes. The so-called 'hysteresis' was clearly observed: The peak shift δ observed on the heating process was different from that on the cooling process. The superlattice reflection below T_C did not lock-in at $\zeta = 0.5$ except for the first heating run, and the peak shift increased as a function of repeat-cycles.

Figure 7(b) shows the temperature dependence of the FWHM of the superlattice reflection along the b^*-axis. The FWHM of the fundamental Bragg reflection as the instrumental resolution is already subtracted. On the first heating process in the commensurate phase,
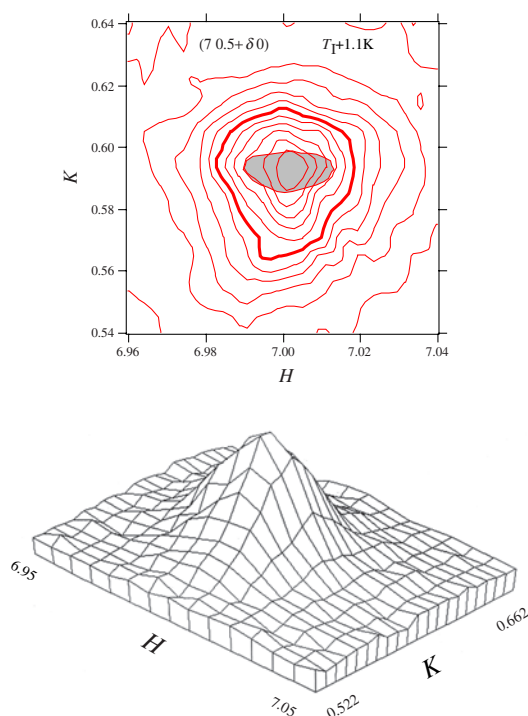
Figure 6. Intensity contour map and a bird's eye view of the diffuse scattering in the reciprocal lattice around (7 0.5+δ 0) recorded at T_I+1.1 K. Contour lines were drawn every 40.5 count per 100 sec. The shaded portion corresponds to the FWHM of a fundamental Bragg reflection representing a resolution function. The thick contour line indicates the FWHM of the observed diffuse scattering.

the corrected FWHM of the superlattice reflection was approximately zero up to T_C, while it exhibited an abrupt jump at T_C. On further heating, the FWHM decreased at once and increased again at T_I. When the sample was cooled again, the temperature dependence of the FWHM on the cooling process was almost the same as that of the first heating process down to T_C. On further cooling below T_C, however, the FWHM increased and showed a finite value. After the one heating-and-cooling cycle, the FWHM in the commensurate phase became larger than that in the incommensurate phase and saturated.

Figure 7(c) shows the temperature dependence of the peak intensity. In the first heating process, the peak intensity decreased abruptly at T_C. On further heating, the peak intensity increased gradually, reaching the maximum at around 26 K, and then decreased gradually. Above T_I, the superlattice reflection became the diffuse scattering and the intensity became almost zero. In the incommensurate phase, temperature dependence of the peak intensities falls on the same line for both the cooling and the heating processes. On the other hand, the intensity in the commensurate phase decreased drastically after the first heating process. This behaviour apparently corresponds to the behaviour of the FWHM.

We conjecture here the origin of the above experimental results: (1) damage of the crystal itself or creation of the misarrangement of the molecular configuration may be occurring; (2) imperfection in the crystal may be caused by the heating-and-cooling cycles or the x-ray irradiation. In order to make this speculation clearer we performed the following experiments.

First, we tested whether the origin was the thermal effect or not. The peak shift δ and the FWHM of the superlattice reflection (7 0.5 0) were observed at 14.4 K after the heating-
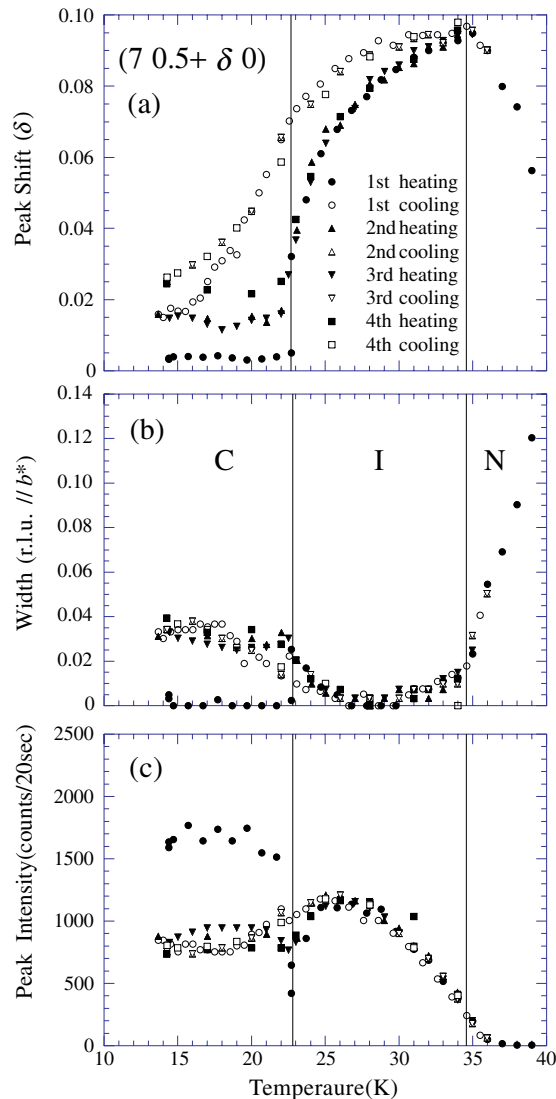
Figure 7. Temperature dependence of the superlattice reflection for successive experimental cycles. (a): peak shift δ, (b): FWHM of the superlattice reflection along the b^*-direction, (c): peak intensity.

and-cooling cycle, such as heating up to 41 K and cooling down to 14.4 K. The experiments were performed 5 times and the sample was not irradiated by x-rays during the heating and the cooling processes. The temperature was increased at a rate of 0.5 K per minute from 14.4 K to 41 K. After keeping the sample for 5 minutes at 41 K, the temperature was decreased at the same rate. The observed peak shift δ and the observed FWHM are shown at each measurement-number of 1–5 in figure 8(a) and figure 8(b), respectively. The FWHM's in figure 8(b) are the raw data and the resolution correction is not performed. As shown in figure 8, they are almost independent of the measurement-number. Thus it is concluded that the thermal treatment or history does not produce the change of the diffraction profile including the width and the peak position.
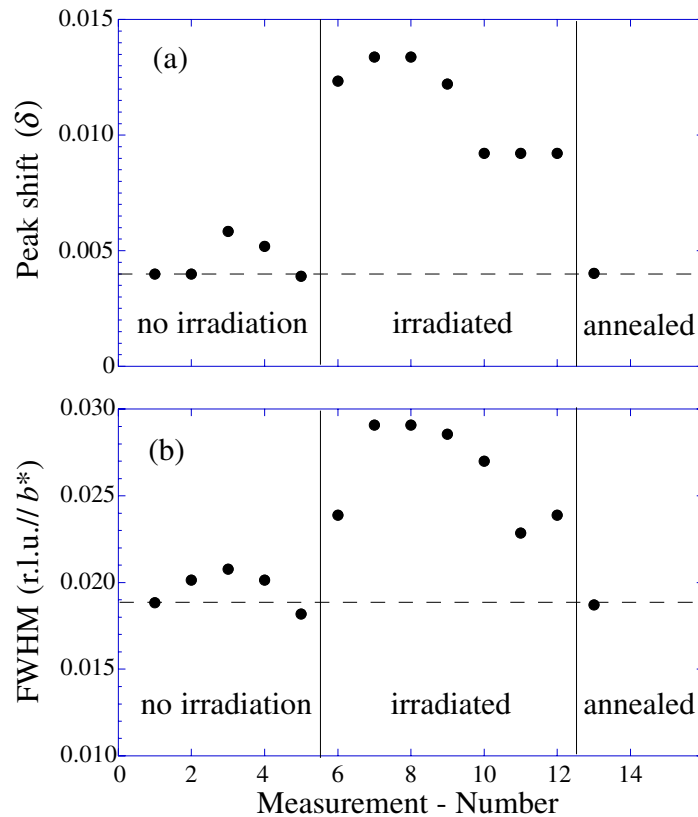
Figure 8. The peak shift δ and the FWHM of the superlattice reflection (7 0.5+δ 0) at 14.4 K after successive experimental procedures (see the text). Dashed lines are guides to the eye.

Next, we investigated the effect of the crystal imperfection introduced by x-ray irradiation. The experimental procedures were as follows. The sample was irradiated with x-rays for 10 hours at 14.4 K and heated to 41 K and then cooled down again to 14.4 K with no irradiation x-rays. We monitored the (7 0.5 0) reflection after this procedure at 14.4 K. These measurements were repeated seven times. The observed peak shift δ and the FWHM of the superlattice reflection at 14.4 K are shown at the measurement-number of 6–12 in figure 8(a) and figure 8(b), respectively. As shown in figure 8, it was found that the peak shift δ and the FWHM increased by the first irradiation of the x-rays. However, after the subsequent irradiation, they were almost the same as those of the first. From those results, we realized that the damage caused by x-ray irradiation increases the δ and FWHM values, and that irradiation only for 10 hours is sufficient to cause the effect. Actually, the peak shift δ had already deviated slightly from the commensurate value of zero even in the first measurement without irradiation (figure 8(a)). This slight shift may be caused by the short time irradiation of x-rays for a sample check.

Finally, an annealing effect will be mentioned here. The irradiated sample was heated up to room temperature and annealed for 3 hours. Then the sample was cooled down to 14.4 K and the peak shift δ and the FWHM of the superlattice reflection were measured. The result is shown as for the measurement-number of 13 in figure 8. The peak shift δ and the FWHM recovered the same value as those of measurement-number 1. Therefore imperfection of the crystal is considered to be restored by annealing at room temperature. The result indicates

that the dissociation of the molecule was not caused by the x-ray irradiation but a small disarrangement of ordering atoms, probably hydrogen atoms, in a crystal occured.

4. Summary and discussion

The phase transitions of deuterated 5-bromo-9-hydroxyhenalenon (d-BrHPLN) at low-temperatures have been investigated by x-ray diffraction experiments. As the first motivation, we synthesized this new material in order to investigate the hydrogen-bond nature and an isotope effect on the transition temperature. Accidentally, we found that the phase transition scheme is the so-called normal-incommensurate-commensurate one. This is probably the first case in which an incommensurate phase has shown such a large isotope effect.

The temperature dependence of lattice constants showed anomalous behaviour at T_I (normal-to-incommensurate) and T_C (incommensurate-to-commensurate). However, the lattice constants did not show a discontinuous change at T_C, despite the first-order nature of the phase transition. The superlattice reflection was found at $(h \ k+0.5 \ 0)$ on the Weissenberg photograph recorded at 14.4 K, and the space group of the lowest phase is determined as $P2_1/c$. Furthermore, we found that the intermediate phase was an incommensurate phase. The peak shift δ, which was defined as a deviation of the superlattice reflection from the commensurate position $(7 \ 0.5+\delta \ 0)$, represents the degree of the incommensurability. The temperature dependence of the peak shift δ showed a thermal hysteresis in the incommensurate phase. The precise peak position of the superlattice reflection slightly deviated from the exact commensurate position even below T_C and was pinned after the experimental cycles. The deviation of the peak position from the commensurate position at the lowest temperature increased after each experimental cycle. Consequently, the origin of the deviation of the pinning position from $\zeta = 0.5$ was found to be caused by the x-ray irradiation.

A similar pinning effect caused by x-ray radiation damage has been also reported in other systems. We compare the present results with those previously reported in other materials. A variety of materials, especially a ferroelectric compound, shows an incommensurate phase transition. Typical examples are $NaNO_2$ and $SC(NH_2)_2$, in which electrical dipole–dipole interaction is important. Long-period phases in thiourea under high electric field are observed by x-ray diffraction [15], and later the results are compared with the data taken by neutron diffraction [16, 17]. Large radiation effects of x-ray beams are discussed. It is noted that the sample irradiated by x-rays retains the radiation damage or radiation-induced defects and the radiation DOSE relates to the lock-in period of unusually long-period structure. It is also reported that no anomalous line shapes could be detected. Other examples of incommensurate materials are A_2BX_4-type compounds. Among them, tetramethylammonium(TMA) compounds are well known to have incommensurate and long-period structures. By x-ray diffraction experiments, drastic radiation damage was found in TMATC-Co [18], and the irradiated sample showed complicated lock-in behaviour. It seems that the damage is kept in a sample and the migration speed of the defect is very slow. This behaviour seems to be similar to the chemical impurity effect in Rb_2ZnCl_4 studied by Mashiyama *et al* [19]. Kiat *et al* also found similar effects in other types of compound [20, 21]. In betaine calcium chloride dihydrate (BCCD), they found complicated lock-in behaviour which was dependent on the irradiation time and the temperature where the sample is irradiated. Time dependence of the misfit parameter for a lock-in transition was also observed in barium sodium niobate [21]. They showed the diffraction profile as a function of time when constant temperature change is interrupted and temperature is holed. Misfit parameter is strongly dependent on the thermal treatment process, cooling or heating, or speed of temperature change. It seems that there are many metastable states energetically similar to

each other. The similar results were found in RbLiSO$_4$ [22], in which diffraction profile and lock-in period are strongly dependent on the path in temperature-electric field space. In this case, no radiation damage was reported.

We emphasize here that the pinning effect of d-BrHPLN is removable by annealing the sample at room temperature and all phenomena are irreversible. This evidence is contradictory to the ordinary lock-in behaviour under irradiation previously reported. Therefore, it is possible that the terminology 'radiation damage' used in this material might be slightly different from those in other materials, or migration speed of defects might be extraordinarily high.

The d-BrHPLN molecule has two energetically equivalent configurations in connection with the hydrogen configuration. Above T_I, the exchange between the two configurations takes place rapidly and the deuterium atom in the hydrogen-bond may be in a disordered state, as shown by NMR and dielectric measurements [11]. The deuterium configuration is believed to be ordered in association with the phase transition at T_I, as also suggested by calorimetric studies [11], although no direct evidence, such as low temperature structures, has been presented for this interpretation. If we take this viewpoint, the origin of the x-ray damage causing the pinning effect may be rationalized as follows. In the commensurate phase below T_C, which may have the ordered deuterium configuration, the x-ray irradiation may induce the configurational exchange shown in figure 1 through excitation of the molecules, and the resultant improper deuterium configurations disturb the ordering patterns. This process may be regarded as generation of the 'defects'. Here we believe that the energy differences of the alternative configurations may be very small in both the incommensurate and the commensurate phases. Finally, we consider the mechanism of the pinning effect caused by such defects. Since the imperfections will be formed locally and randomly in a crystal, they are not even detectable just after creation. However, once such defects are introduced in the crystal, the ordering process of the deuterium configurations in the incommensurate phase will be affected by the 'embryo' and the size of the coherently ordered region will decrease. This process may lead to the broad scattering profile and the pinning effect below T_C. We also note that the picture presented here is consistent with the computer simulation in which discommensuration is introduced randomly in a crystal [23]. The pinning mechanism mentioned here is still our speculation, and we consider that the structure analysis at the low-temperature phase is important to discuss quantitatively such a pinning effect and the mechanism of the phase transition, especially the large isotope effect. The precise structure analysis and neutron scattering experiments are now underway.

Acknowledgments

References

[1] Blinc R 1960 *J. Phys. Chem. Solids* **13** 204
[2] Tokunaga M and Matsubara T 1966 *Prog. Theor. Phys.* **35** 581
[3] Ichikawa M, Motida K and Yamada N 1987 *Phys. Rev.* **B 36** 874
[4] Noda Y, Uchiyama S, Kafuku K, Kasatani H and Terauchi H 1990 *J. Phys. Soc. Japan* **59** 2804
[5] Noda Y, Kasatani H, Watanabe Y, Terauchi H and Gesi K 1990 *J. Phys. Soc. Japan* **59** 3249
[6] Noda Y and Kasatani H 1991 *J. Phys. Soc. Japan* **60** 13
[7] Noda Y, Kasatani H, Watanabe Y and Terauchi H 1992 *J. Phys. Soc. Japan* **61** 905

 [8] Noda Y, Tamura I, Nakao H, Matsuo R and Kuroiwa Y 1994 *J. Phys. Soc. Japan* **63** 1803
 [9] Gesi K 1980 *J. Phys. Soc. Japan* **48** 886
[10] Bondybey V E, Haddon R C and English J H 1984 *J. Chem. Phys.* **80** 5432
[11] Mochida T, Izuoka A, Sugawara T, Moritomo Y and Tokura Y 1994 *J. Chem. Phys.* **101** 7971
[12] Moritomo Y, Tokura Y, Mochida T, Izuoka A and Sugawara T 1995 *J. Phys. Soc. Japan* **64** 1892
[13] Noda Y, Tamura I, Kuroiwa Y, Mochida T and Sugawara T 1994 *J. Phys. Soc. Japan* **63** 4286
[14] Kuroiwa Y, Tamura I, Ohe F, Jidaisho H, Akiyama K and Noda Y 1995 *J. Appl. Crystallogr* **28** 341
[15] Moudden A H, Moncton D E, and Axe J D 1983 *Phys. Rev. Lett.* **51** 2390
[16] Durand D, Denoyer F, Currat R and Vettier C 1984 *Phys. Rev.* **B 30** 1112
[17] Andre G, Durand D, Denoyer F, Currat R and Moussa F 1987-II *Phys. Rev.* **B 35** 2909
[18] Fjaer E, Cowly R A, and Ryan T W 1985 *J. Phys. C: Solid State Phys.* **18** L41
[19] Mashiyama H, Tanisaki S and Hamano K 1982 *J. Phys. Soc. Japan* **51** 2538
[20] Kiat J M, Calvarin G, Chaves M R, Almeida A, Klopperpieper A and Albers J 1995-II *Phys. Rev.* B **52** 798
[21] Kiat J M, Calvarin G and Schneck J 1994-II *Phys. Rev.* B **49** 776
[22] Konishi H, Noda Y and Yamada Y 1985 *Japan. J. Appl. Phys.* **S24-2** 338
[23] Noda Y, Takimoto M and Yamada Y 1984 *Annual Meeting of the Physical Society of Japan* No 2 p 97